



# II

## Publication II

S. Sillanpää and M. Heinonen, The varying effect of natural convection on shear stress rate on cylindrical surfaces, *Experimental Thermal and Fluid Science* **32**, 459 - 466 (2007).

© 2007 Elsevier Inc

Reprinted with permission from Elsevier.

# The varying effect of natural convection on shear stress rate on cylindrical surfaces

S. Sillanpää \*, M. Heinonen

*Centre for Metrology and Accreditation (MIKES), P.O. Box 9, FI-02151 Espoo, Finland*

Received 17 November 2006; received in revised form 19 April 2007; accepted 24 May 2007

## Abstract

In a dynamic weighing gas mass flow measurement, the gas mass flow rate is continuously determined by weighing a gas mass loss from a gas cylinder as a function of time. In this measurement method, the temperature difference between the wall of the gas cylinder and ambient air cannot be avoided. Due to natural convection flow, a shear stress appears on the wall of the cylinder. Because of the dynamic nature of the method, the shear stress rate varies as a function of time during the measurement period. In this paper, the magnitude and effect of the variable shear stress was studied theoretically and experimentally. Obtained results showed good agreement between the theory and experiments.

© 2007 Elsevier Inc. All rights reserved.

*Keywords:* Natural convection; Shear stress; Dynamic weighing

## 1. Introduction

Natural convection flow originates when a body force acts on a fluid containing density gradients. The net effect is a buoyancy force, which drives the fluid motion. In this article, the dynamic effect of natural convection on forces acting on cylindrical surfaces is studied. Here, the density gradient is due to a temperature gradient and the gravity is the body force.

In the most accurate small gas flow measurements, the mass flow is determined by continuously weighing the gas mass loss from a gas cylinder as a function of time (see e.g. [1–5]). In these applications, varying convection flow of ambient air on the wall of a gas cylinder can be a significant source of measurement uncertainty. The effects of forced convection due to laboratory ventilation and natural convection due to thermal disturbances of surroundings are minimized by shields around the weighing system. Air flow along the cylinder surface, however, cannot be prevented if the cylinder is not in a thermal equilibrium with

the ambient. The temperature gradient between the wall of the gas cylinder and ambient air causes air density variations in the boundary layer of the gas cylinder.

If the velocity profile of the flow is known, for air as a Newtonian fluid, the shearing stress at the cylinder wall ( $\tau_w$ ) and the rate of shearing strain are linked together with a relationship of the form

$$\tau_w = \mu \left. \frac{du}{dy} \right|_w, \quad (1)$$

where  $\mu$  is an absolute viscosity and  $du/dy$  is velocity gradient, respectively. As can be seen, temperature changes of the cylinder wall during measurements alter the natural convection flow and shearing stress.

The heat transfer based on the natural convection flow has been studied widely. However, research results relating to the shearing stress caused by the flow field are reported mainly by mass metrologists. In mass measurements, the thermal equilibrium between the weighed object and surrounding air cannot be totally achieved. In [6], the effect of free convection on the apparent mass of 1 kg mass standards has been studied theoretically and experimentally

\* Corresponding author. Tel.: +358 10 6054 433; fax: +358 10 6054 499.  
E-mail address: [sampo.sillanpaa@mikes.fi](mailto:sampo.sillanpaa@mikes.fi) (S. Sillanpää).

## Nomenclature

$A_w$	surface area, m <sup>2</sup>	$x$	coordinate, m
$c_i$	sensitivity coefficient	$y$	coordinate, m
$c_p$	specific heat, J kg <sup>-1</sup> K <sup>-1</sup>	$y_i$	estimate of the measurand
$F_w$	force, N		
$f$	dimensionless similarity variable	<i>Greeks</i>	
$g$	acceleration due to gravity, m s <sup>-2</sup>	$\alpha$	sensitivity coefficient of the balance, thermal diffusivity, m <sup>2</sup> s <sup>-1</sup>
$Gr_x$	local Grashof number	$\beta$	coefficient of thermal expansion, K <sup>-1</sup>
$I$	indication of a balance, mg	$\Delta$	characteristic difference
$k$	thermal conductivity, W m <sup>-1</sup> K <sup>-1</sup>	$\delta$	characteristic correction
$m$	mass, kg	$\varepsilon$	emissivity
$\delta m_T$	contribution to the indication of a balance due to disruptive force, mg	$\eta$	dimensionless similarity parameter
$m, n$	dimensionless constants	$\Theta$	dimensionless temperature difference
$\delta m_c$	difference in the indication of a balance, mg	$\rho, \rho_a$	density and air density, respectively, kg m <sup>-3</sup>
$Pr$	Prandtl number	$\tau_w$	shear stress, Pa
$q_w$	heat flux, W m <sup>-2</sup>	$\mu$	absolute viscosity, N s m <sup>-2</sup>
$Ra_x$	local Rayleigh number	$\nu$	kinematic viscosity, m <sup>2</sup> /s
$T_w$	wall temperature, K		
$T_\infty$	ambient temperature, K	<i>Abbreviations</i>	
$t$	time, s	CFD	Computational Fluid Dynamics
$u$	uncertainty, velocity along a surface, m s <sup>-1</sup>	GUM	Guide to the Expression of Uncertainty in Measurement
$u_c$	combined standard uncertainty	MIKES	Centre for Metrology and Accreditation
$v$	velocity normal to surface, m s <sup>-1</sup>		

by Gläser and Do. The theory was based on the work by Schmidt et al. [7]. As a conclusion, Gläser and Do found that the theory of free convection along a vertical isothermal plate can be applied to estimate the magnitude of a force caused by natural convection. The more advanced study of the effect of temperature differences in weights was presented by Gläser in [8]. He developed physical models taking into account different heat transfer processes and convective forces of flowing air acting on the weight.

Decreasing costs of computer time and development of computational fluid dynamic (CFD) codes inspired Mana et al. [9] to study the convection phenomenon numerically. By using experimentally determined boundary and initial conditions for air temperature, they calculated successfully a flow field around a stainless steel 1 kg mass standard and a silicon sphere with the same nominal mass.

In all earlier studies, the shear stress rate on the surface was assumed to be constant during observations. Investigations reported here are focused in time dependent natural convection affecting cylindrical surfaces, for example a gas cylinder of a dynamic gravimetric gas flow standard. In this case, the shear stress rate is a function of time during the measurement process and changes are larger than in traditional mass calibrations due to handling of the cylinder and decreasing pressure in it. Also the dynamic measurement method and the use of cylinders with different surface types make the gas flow standard more sensitive to natural convection.

To minimize the changes in shear stress, the surface should be in thermal equilibrium with the ambient air

(no heat transfer) or the temperature gradient between the surface and ambient air constant during some observation period (constant heat transfer). If the heat transfer between the surface and ambient varies, the shear stress on the surface is not constant anymore. The aim of the work reported here is to develop a theoretical model for estimating the natural convection effect in a primary mass flow standard and to study its contribution to overall uncertainty. The model was validated by gravimetric measurements. In this paper, first the theoretical analysis of varying shear stress induced by natural convection flow is presented. Based on the theory, the shearing stresses are calculated numerically. Two different cylinder set-ups are studied: a cylinder standing at vertical and horizontal position on the balance. The theory of two dimensional steady laminar free convection flow for a vertical isothermal surface is applied to the vertical position. The same theory applied for a rounded surface was used for the horizontal cylinder position. The effect was studied experimentally with the gas mass flow measurement system at the Centre for Metrology and Accreditation (MIKES). An uncertainty calculation for the shear stress difference measurement as a function of temperature is also presented.

## 2. Theoretical analysis

The wall of the gas cylinder standing vertically can be treated as a vertical plate in two dimensions, as in Fig. 1. The flow along the wall of the gas cylinder is assumed lam-

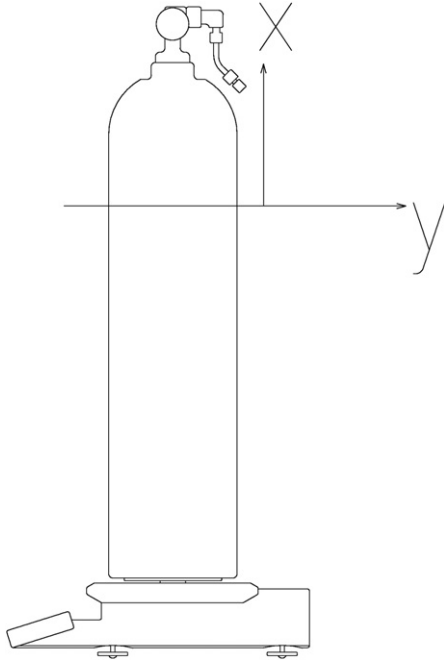


Fig. 1. The coordinate system for a vertical gas cylinder.

inar, steady and constant in terms of property conditions. The gravitational force acts in the negative  $x$ -direction and the fluid is also assumed to be incompressible. If  $\Delta T$  is a characteristic temperature difference between the cylinder wall and ambient air  $\Delta T = T_w - T_\infty$ , then in the limiting case,  $\Delta T/T_\infty = 0$ , all physical properties reduce to their values at  $T_\infty$ . Applying the Boussinesq approximation, air density variations can be assumed so small that they can be neglected [10,11].

Assuming that the surface roughness of a cylindrical surface will not affect to the stability of the flow, then the basic equations for boundary layer for laminar natural convection are

$$\frac{\partial u}{\partial x} + \frac{\partial v}{\partial y} = 0, \quad (2)$$

$$u \frac{\partial u}{\partial x} + v \frac{\partial u}{\partial y} = g\beta(\Delta T) + \nu \frac{\partial^2 u}{\partial y^2}, \quad (3)$$

$$u \frac{\partial T}{\partial x} + v \frac{\partial T}{\partial y} = \alpha \frac{\partial^2 T}{\partial y^2}. \quad (4)$$

In Eqs. (2)–(4)  $u$  is the velocity component along the plate and  $v$  corresponding component normal to it as in Figs. 1 and 3. The buoyancy parameter  $g\beta$  depends on the flowing fluid ( $\beta = (d\rho_a/dT)/\rho_a$ ), whereas the thermal diffusivity  $\alpha = k/(\rho c_p)$  is assumed to be constant and  $\nu$  is kinematic viscosity, respectively. The Eqs. (2)–(4) are known as the continuity equation, momentum equation and energy equation, respectively. Assuming that there are no slip or temperature jump at the wall and fluid is at rest under ambient temperature at infinity, the following boundary and initial conditions can be used:

$$u(x, 0) = v(x, 0) = u(x, \infty) = 0, \quad (5)$$

$$T(x, 0) = T_w(x) \quad T(x, \infty) = T_\infty = \text{constant}. \quad (6)$$

If  $\Delta T < 0$ , the buoyancy driven flow is downward and the leading edge is at the top of the wall of the cylinder. If  $\Delta T > 0$ , the situation is opposite.

For a vertical plate flow, velocity and thickness scales were deduced in [7,12], where following similarity parameters were defined:

$$\eta = \left( \frac{Gr_x}{4} \right)^{\frac{1}{4}} \frac{y}{x}, \quad (7)$$

$$Gr_x = \frac{\beta g(\Delta T)x^3}{\nu^2}, \quad (8)$$

$$u = 2[x\beta g(\Delta T)]^{\frac{1}{2}} f'(\eta), \quad (9)$$

$$v = \left[ \frac{\beta g(\Delta T)\nu^2}{4x} \right]^{\frac{1}{4}} (\eta f' - 3f), \quad (10)$$

$$\Theta = \frac{T - T_\infty}{\Delta T}. \quad (11)$$

In Eq. (8)  $Gr_x$  is the local Grashof number which indicates the ratio of the buoyancy force to the viscous force acting on the fluid. Variables in Eqs. (7)–(11) satisfy the continuity equation explicitly and reduce the momentum and energy equations to a group of two coupled nonlinear differential equations [10,13].

$$f''' + (3 + m + n)ff'' - 2(1 + m + n)f'^2 + \Theta = 0, \quad (12)$$

$$\Theta'' + (3 + m + n)Prf'\Theta' - 4mPrf'\Theta = 0. \quad (13)$$

In Eqs. (12) and (13), primed quantities indicate differentiation with respect to  $\eta$ , and  $Pr$  is Prandtl number. Variables  $f$  and  $\Theta$  are functions of  $\eta$  with boundary and initial conditions

$$f(0) = f'(0) = f'(\infty) = 0, \quad (14)$$

$$\Theta(0) = 1 \quad \Theta(\infty) = 0. \quad (15)$$

The wall temperature is assumed to obey the power law. Therefore, the standard cases are determined by  $m = 0$  ( $T_w$  is a constant) and  $m = 1/5$  (heat flux  $q_w$  is a constant). Each value of  $n$  corresponds to a particular body contour. For  $n = 0$ , a flat plate is obtained, while the value  $n = 1$  corresponds to the stagnation-point flow along a rounded surface, for example a circular cylinder as in Fig. 3.

The flow field driven by natural convection can now be calculated for different types of cylindrical surfaces by solving numerically Eqs. (12) and (13) with the boundary and initial conditions (14) and (15).

When the velocity field around the cylinder is calculated with assumption of the fluid as Newtonian, the shearing stress  $\tau_w$  on the cylinder wall can be calculated according to

$$\tau_w = \rho\nu \frac{du}{dy} = \frac{2\mu}{x} [x\beta g(T_w - T_\infty)]^{\frac{1}{2}} \left( \frac{Gr_x}{4} \right)^{\frac{1}{4}} f''(0). \quad (16)$$

The net force  $F_w$  caused by natural convection is calculated by integrating the shear stress over the cylinder surface

$$F_w = \int \tau_w dA_w. \tag{17}$$

The mass difference of an object  $\delta m_c$ , is calculated by dividing the Eq. (17) by the acceleration due to gravity:  $\delta m_c = F_w/g$ .

The shear stress rate is a function of temperature difference  $\tau_w = \tau_w(\Delta T)$ . In a time dependent situation, the temperature difference is a function of time  $\Delta T = \Delta T(t)$ . The mean shear stress difference affecting on a surface at some arbitrary time interval from  $t'$  to  $t$  can be calculated as the time average

$$\overline{\Delta \tau_w} = \frac{1}{t - t'} \int_{t'}^t \tau_w(\Delta T(t)) dt. \tag{18}$$

### 3. Results and discussion

#### 3.1. Numerical solution

Calculations were made for a case, where an aluminium cylinder with vertical wall height of 590 mm and outer diameter of 152 mm was surrounded by air. The calculation of the flow induced by natural convection was based on the numerical solution of Eqs. (12) and (13) with initial and boundary conditions (14) and (15). The following numerical values were used in the calculations:  $\rho_a = 1.2 \text{ kg m}^{-3}$  [15],  $\nu = 1.8 \times 10^{-5} \text{ m}^2 \text{ s}^{-1}$ ,  $\beta g \nu^{-2} = 1.5 \times 10^5 \text{ K}^{-1} \text{ m}^{-3}$  and  $Pr = \mu c_p k^{-1} = 0.72$  [12]. The buoyancy volume of the cylinder was estimated to be  $10 \text{ dm}^3$ . The finite difference code, which implements the three-stage Lobatto IIIA formula, was used. Mesh selection and error control were based on the residual of the continuous solution.

The numerical solution was obtained for situation  $m = 0$ , where the wall was supposed to be isothermal. Velocity profiles at 10 different values of  $\Delta T$  at five different heights (see Figs. 2 and 3) at the boundary layer of the gas cylinder were first solved. Examples of theoretical velocity profiles at the temperature difference of 10 K are presented at five different heights of vertical and horizontal cylindrical surfaces in Figs. 4 and 5. It can be noticed that calculated velocity profiles in Figs. 4 and 5 at the temperature difference of 10 K and Prandtl number 0.72 follow the classical numerical solution of Eqs. (12) and (13), reported by Ostrach [14].

$\Delta \tau_w$  was calculated as a function of temperature difference for vertical and horizontal cylinder positions according to Eq. (18). Fig. 6 presents the calculation results for the effect of natural convection on shear stress difference on a cylindrical surfaces as a function of temperature difference. The net mean shear stress difference constitutes of contributions calculated in the five observation points

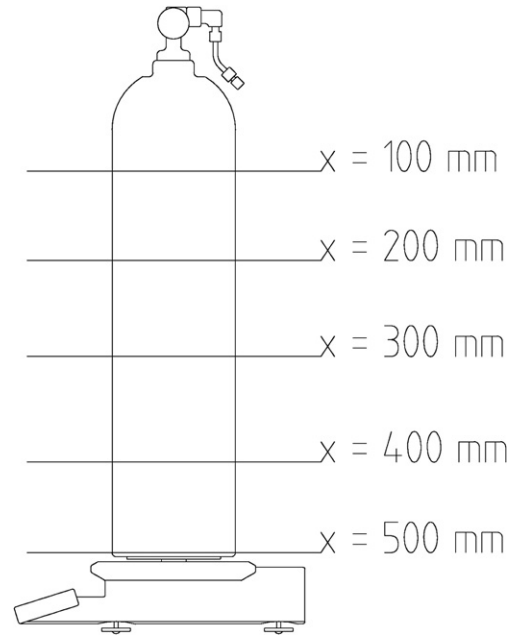


Fig. 2. Calculation points for a vertical gas cylinder. The insulation plate is not shown in the figure.

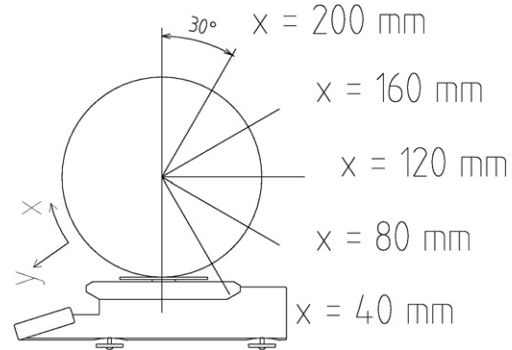


Fig. 3. The coordinate system and calculation points for a horizontal gas cylinder. The insulation plate is not shown in the figure.

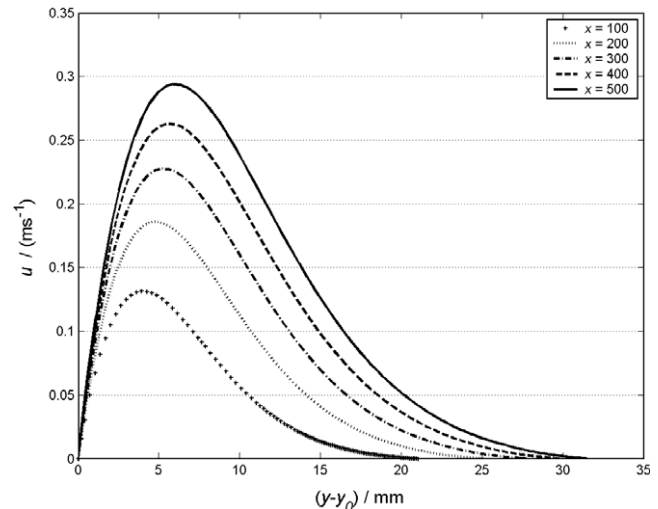


Fig. 4. Example of calculated velocity profiles for the vertical gas cylinder at a temperature difference of 10 K. Small ticks:  $x = 100 \text{ mm}$ , dotted line:  $x = 200 \text{ mm}$ , dash-dot line:  $x = 300 \text{ mm}$ , dashed line:  $x = 400 \text{ mm}$  and solid line:  $x = 500 \text{ mm}$ .

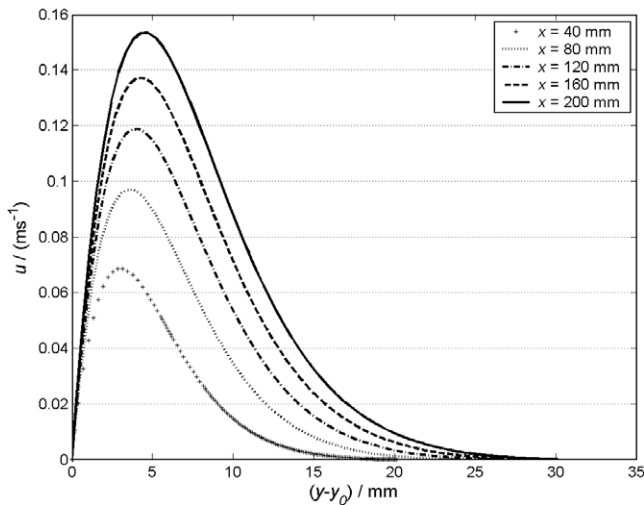


Fig. 5. Example of calculated velocity profiles for the horizontal gas cylinder at a temperature difference of 10 K. Small ticks:  $x = 40$  mm, dotted line:  $x = 80$  mm, dash-dot line:  $x = 120$  mm, dashed line:  $x = 160$  mm and solid line:  $x = 200$  mm.

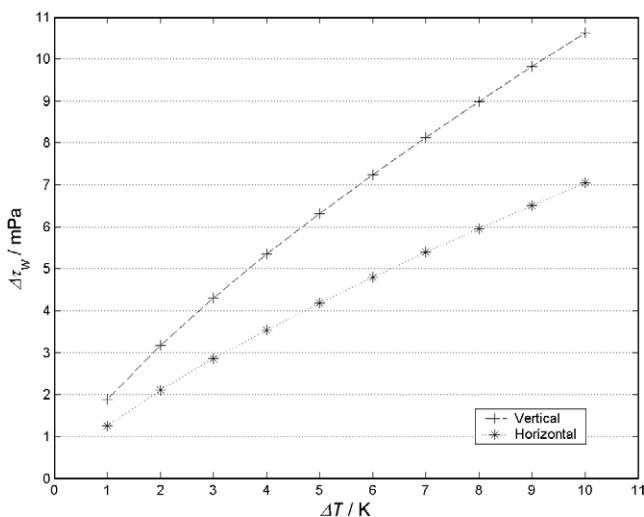


Fig. 6. Theoretical effect of natural convection for a vertical (+) and horizontal (\*) gas cylinder.

showed in Figs. 2 and 3. The difference between horizontal and vertical set-ups in the development of the shear stress rate can be seen in the figures.

### 3.2. Measurements with a vertical cylinder

The effect of natural convection was studied experimentally with the MIKES primary gas mass flow measurement system. The cylindrical surface is a gas cylinder placed on the balance. The indication of the balance and the surface temperature of the cylinder are monitored continuously during weighing as a function of time. Changes in shear stress on the wall of the cylinder induce direct changes in the air buoyancy corrected balance indication.

Before starting measurements, the gas cylinder was heated roughly 10 K above the ambient temperature.

Temperature gradients at the wall of the cylinder were let to stabilise about 45 min. Heating of the cylinder was chosen instead of cooling to avoid the risk of water condensation on the surface of the cylinder, (the relative humidity of air in the laboratory was 50% corresponding to the dew-point temperature of 9.5 °C at the ambient temperature of 20 °C). After an appropriate stabilisation time, the cylinder was placed on the weighing pan of a balance with a maximum load of 10,100 g and scale interval of 1 mg.

Three measurement cycles were performed. In the cycles 1 and 3, the wall temperature of the cylinder as a function of time was monitored with a small thermistor attached on the wall. In the cycle number 2, the thermistor was detached and the wall temperature was observed with a thermographic camera. A plate made of thermally resistive material was placed between the weighing pan and the gas cylinder. The diameter of the plate was larger than the diameter of the cylinder and its boundary layer together. The purpose of the plate was to minimize the effect of heat conduction from the gas cylinder to the balance and an upward convection flow caused by the balance. After the stabilisation time, the wall of the cylinder was assumed to be isothermal, the balance was adjusted and the measurement cycle was started.

During the cycles 1 and 3, indications of the balance and corresponding temperature and time readings were recorded by a computer. In the measurement cycle number 2, the surface temperature of the cylinder was observed with the thermographic camera and the thermistor was not in use. This was done to examine, if there were any parasitic forces caused by the connection wire of the thermistor. The thermographic measurement also gave information about possible thermal gradients at the cylinder wall. In pictures of Fig. 7, the mean temperatures taken from the middle part of the gas cylinder are presented in five different points in time during the cylinder cooling. Each colour illustrates particular temperature, respectively. Warmer parts are shown in red and cooler in blue colour.<sup>1</sup> The cooling of the cylinder from 28 °C to 24.2 °C took 2880 s. The colour of the surface was black matte. In thermographic measurements, the emissivity of the surface was assumed to be  $\varepsilon = 0.95$ . The purpose of the measurements was to study changes in temperature differences in time against some reference temperature, so the absolute determination of emissivity was not critical.

In Fig. 8, all points from three measurement cycles are compared with the calculated solution based on the theory, showing measured changes in shear stress difference as a function of temperature. Line of dots and dashes shows the calculated shear stress rate as a function of temperature. Marked points illustrate experimental results from measurement cycles 1–3.

<sup>1</sup> For interpretation of color in Fig. 7, the reader is referred to the web version of this article.



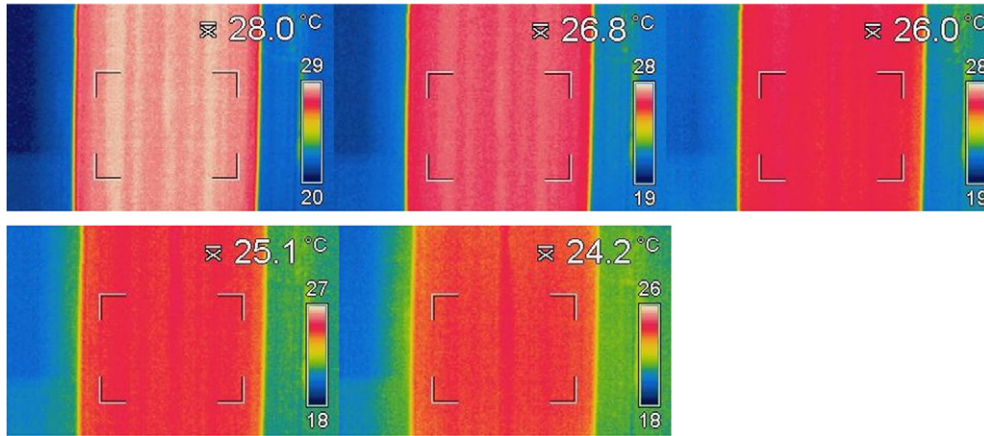


Fig. 7. The surface temperature of the gas cylinder was monitored also with a thermographic camera in one of the measurement cycles. Mean temperatures at the cornered area, taken from the middle part of the cylinder, are shown in the top right corner of each picture.

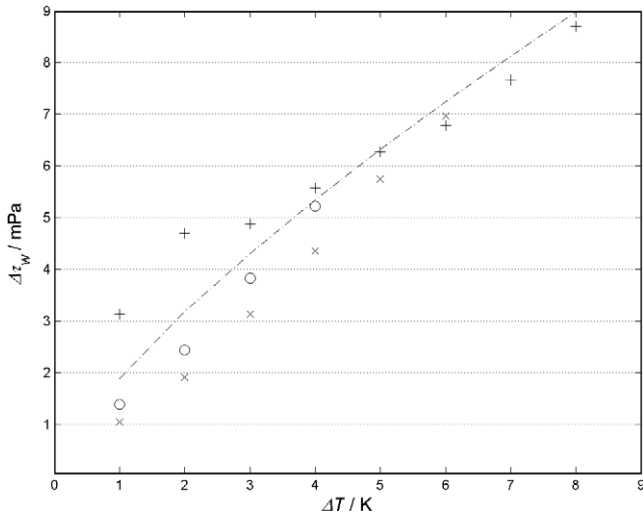


Fig. 8. Measurement results and theoretical curve for the vertical gas cylinder. +: measurement 1, O: measurement 2, x: measurement 3. Dash-dot-line: theoretical curve.

### 3.3. Uncertainty calculations for the shear stress difference and the cylinder wall temperature measurements

The shear stress difference can be obtained by dividing the measured force difference ( $\Delta F$ ) by the vertical surface area of a studied object ( $A_w$ )

$$\Delta\tau_w = \frac{\Delta F}{A_w} = \frac{g\Delta m}{A_w} = \frac{g}{A_w} \frac{\Delta I - \Delta\delta m_T}{\alpha \left(1 - \frac{\rho_a}{\rho_t}\right)}, \quad (19)$$

where  $\Delta m$  is the measured mass difference of the gas cylinder,  $\rho_a$  density of surrounding air,  $\rho_t$  density of the gas cylinder,  $\Delta I$  difference in indication of the balance during the measurement,  $\Delta\delta m_T$  error in the balance indication difference due to the connecting wire of the thermistor and other disturbances,  $\alpha = (1 - \rho_{a0}/\rho_{r0})^{-1}$ ,  $\rho_{a0} = 1.2 \text{ kg/m}^3$  and  $\rho_{r0} = 8000 \text{ kg/m}^3$ . The measurement uncertainty in the

experimental determination of  $\Delta\tau_w$  can be derived from the uncertainties of the parameters in Eq. (19) according to the method presented in Guide to the Expression of Uncertainty in Measurement (GUM) [16]. The uncertainty of  $\Delta I$  includes contributions from the non-linearity and resolution of the balance. Based on the estimated uncertainties from ambient air temperature, pressure and humidity, the uncertainty of air density was estimated to be  $0.1 \text{ kg/m}^3$  at maximum. The uncertainties of  $\rho_t$  and  $\Delta\delta m_T$  were estimated to be 10% ( $94 \text{ kg/m}^3$ ) at maximum and 5 mg at maximum, respectively. The acceleration due to gravity ( $g = 9.819098 \text{ ms}^{-2}$ ) is known with an expanded uncertainty of  $4 \times 10^{-6} \text{ ms}^{-2}$ , which is so small that it can be neglected. As an example, uncertainty budgets for  $\Delta T = 1 \text{ K}$  and  $\Delta T = 8 \text{ K}$  are presented in Table 1.

When estimating the standard uncertainty of the wall temperature of the cylinder, the indication of the thermistor, calibration correction, resolution and non-isothermality of the wall were considered. Applying the GUM method, the combined standard uncertainty for the temperature measurement was estimated to be 0.65 K. By taking into account the uncertainty contributions from shear stress difference and wall temperature measurement, the combined standard uncertainty is from 0.7 MPa/K at  $\Delta T = 1 \text{ K}$  to 1.3 MPa/K at  $\Delta T = 8 \text{ K}$ .

### 3.4. Assessment of results

Transition from laminar to turbulent flow in a free convection boundary layer depends on the relative magnitude of the buoyancy and viscous forces in the fluid. Typically, this is characterised in terms of Rayleigh number

$$Ra_x = Gr_x Pr. \quad (20)$$

For a vertical and a horizontal cylinder positions, the critical value for Rayleigh number is  $Ra_x = 10^9$  [11]. For Rayleigh number smaller than the critical value, boundary layer is assumed to be laminar. Based on the numerical solution, the maximum Rayleigh number for the vertical

Table 1

Example of an uncertainty budget for shear stress difference measurement at  $\Delta T = 1$  K and  $\Delta T = 8$  K

$y_i$	Unit	$\Delta T = 1$ K		$\Delta T = 8$ K	
		$u(y_i)^a$	$c_i u_i(y_i)^b$	$u(y_i)^a$	$c_i u_i(y_i)^b$
$\Delta I$	kg	$7.01 \times 10^{-7}$	0.29	$7.01 \times 10^{-7}$	0.29
$\rho_a$	kg/m <sup>3</sup>	0.06	$1.52 \times 10^{-5}$	0.06	$1.14 \times 10^{-4}$
$\rho_t$	kg/m <sup>3</sup>	108	$3.65 \times 10^{-5}$	109	$2.73 \times 10^{-4}$
$\Delta \delta m_T$	kg	$2.89 \times 10^{-6}$	0.12	$2.89 \times 10^{-6}$	0.12
$A_w$	m <sup>2</sup>	0.14	0.14	0.14	1.07
$u_c(\tau_w)^c$	MPa		0.34		1.1
$U(k = 2)^d$	MPa		<b>0.7</b>		<b>2.2</b>

<sup>a</sup> Standard uncertainty of  $y_i$ .

<sup>b</sup> Contribution to the combined standard uncertainty in MPa.

<sup>c</sup> Combined standard uncertainty.

<sup>d</sup> Expanded uncertainty at approximately 95% confidence level.

cylinder was  $1.77 \times 10^8$  and for horizontal cylinder  $1.18 \times 10^7$  at the temperature difference of 8 K. Thus, the assumption of laminar boundary layer was tenable.

The assumption of an isothermal cylinder wall was shown correct based on the thermographic results: As can be seen from Fig. 7, there were not noticeable temperature variations on the surface of the cylinder. When comparing measurement results and calculated curve, as in Fig. 8, it can be seen that the measurement data follows quite well the presented theory. The largest deviations can be found at temperature cycle differences from 1 K to 3 K in the measurement cycle number 1. These differences are probably due to some non-isothermal areas on the cylinder wall or an upward convection flow caused by the balance.

An interesting conclusion could be drawn by comparing the results derived for cylinders in different positions: Let assume that there are two similar isothermal cylinders at the same temperature.  $\Delta \tau_w$  for the horizontal cylinder is approximately 29% less than for the vertical cylinder set-up. This is due to lower vertical height of the gas cylinder. Density gradients on the boundary layer on the gas cylinder are situated in a smaller vertical height, which reduces the velocities of free convection flow.

When comparing the development of shear stress rates between vertical and horizontal cylinder positions at five calculation points, some differences can be seen. For the vertical position with  $\Delta T = 10$  K, the shear stress at the first calculation point is 67% of the maximum value at the fifth point. Then it grows to 79%, 88%, 94% and finally to 100%. Corresponding percentages for the horizontal position are 66%, 71%, 76%, 84% and 100%. So, at the vertical cylinder position the shear stress grows faster at the nearest calculation points from the leading edge. For the horizontal position the situation is opposite. The trend can also be discerned in Fig. 9.

In the dynamic weighing gas mass flow measurement process, the effect of natural convection flow depends on the temperature of the wall of the gas cylinder. The wall temperature depends on the heat exchange between the gas and the wall of the cylinder and between the wall and ambient air. Decreasing gas pressure inside the cylinder

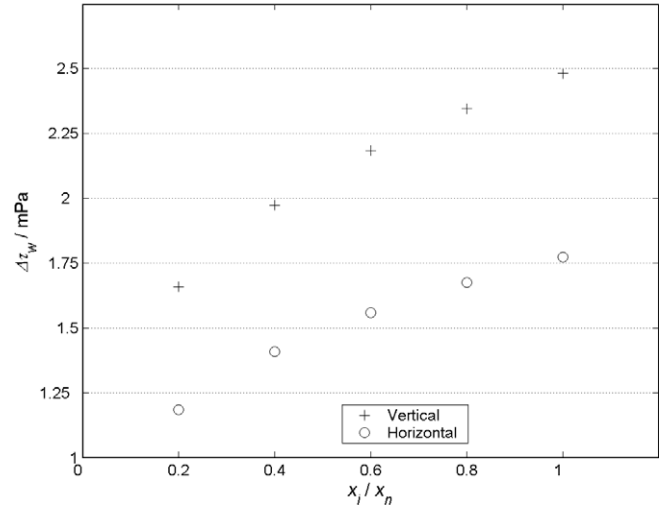


Fig. 9. Shear stress of the gas cylinder at the calculation points as a function of dimensionless  $x$  - coordinate. +: Vertical position, O: horizontal position.

induces the temperature difference between the cylinder wall and ambient air.

The wall temperature of the gas cylinder varies nonlinearly during the gas mass flow measurement. To obtain the gas mass loss from the cylinder as precise as possible, the correction caused by the change in the shear stress rate on the cylinder wall has to be applied. The net effect of shear stress to the gas mass flow rate is

$$\delta \dot{m}_c = \frac{d}{dt} \int \left[ \frac{1}{g(t-t')} \int_{t'}^t \tau_w(\Delta T(t)) dt \right] dA. \quad (21)$$

To examine the order of magnitude of effect of varying shear stress difference to the gravimetric gas mass flow standard, let us consider a gas cylinder with the dimensions presented above. It is placed on the vertical position and

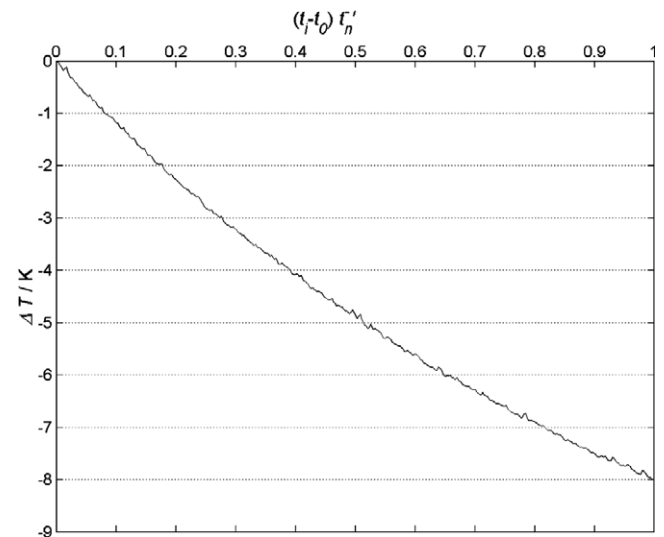


Fig. 10. An example of temperature difference of a gas cylinder wall during a hypothetical gas mass flow measurement as a function of dimensionless time.



the temperature of the wall of the cylinder cools down isothermally 8 K ( $\Delta T < 0$ ) during one measurement cycle, as in Fig. 10. If the gas mass flow rate is 1 mg/s, the effect of varying shear stress to the measurement result is  $-0.22$  mg/s according to Eq. (21). This is equivalent to the relative effect of  $-22\%$ . At the mass flow rate 625 mg/s the effect is  $-2.8$  mg/s and  $-0.4\%$ , respectively. For the horizontal gas cylinder position, corresponding results are  $-0.16$  mg/s and  $-16\%$  for the flow rate 1 mg/s and  $-2.0$  mg/s and  $-0.32\%$  for the flow rate 625 mg/s. At MIKES, the primary gravimetric gas mass flow standard operates with a standard uncertainty from 0.15% to 0.40%. Thus, the temperature variations may induce a significant large contribution to the indication of the mass flow standard.

#### 4. Conclusion

The effect of varying natural convection on shear stress difference on cylindrical surfaces is studied theoretically and experimentally. The theory is based on the solution of laminar boundary layer equations using the similarity variables. If the shear stress varies as a function of time, its effect can be estimated as a time average over some observation period from  $t'$  to  $t$ .

The effect was studied experimentally using the dynamic gravimetric gas mass flow primary standard at MIKES. In that system, the variations in the shear stress on a cylindrical surface can be directly seen as a change in the indication of a balance. Obtained experimental results agreed well with results calculated with the presented theory.

As an application of the theory, the method was implicated to dynamic gravimetric gas mass flow measurement. With help of the theory, it was possible to correct the measurement result and estimate the total effect of varying shear stress on gas mass flow using time averaging.

As a conclusion, the theory can be used for estimating the varying shear stress difference on cylindrical surfaces caused by changing natural convection flow.

#### References

- [1] S. Sillanpää, B. Niederhauser, M. Heinonen, Comparison of the primary low gas flow standards between MIKES and METAS, *Measurement* 39 (2006) 26–33.
- [2] D. Knopf, Continuous dynamic-gravimetric preparation of calibration gas mixtures for air pollution measurements, *Accredit. Qual. Assur.* 6 (2001) 113–119.
- [3] B. Niederhauser, J. Barbe, Bilateral comparison of primary low gas flow standards between the BNM-LNE and METAS, *Metrologia* 39 (2002) 573–578.
- [4] D. Knopf, W. Richter, Highly accurate gas mixtures by dynamic gravimetric method, *PTB-Mitteilungen* 108 (1998) 201–205.
- [5] D. Knopf, J. Barbe, W. Richter, A. Marschall, Comparison of the gas mass flow calibration systems of the BNM-LNE and the PTB, *Metrologia* 38 (2001) 197–202.
- [6] M. Gläser, J.Y. Do, Effect of free convection on the apparent mass of 1 kg mass standards, *Metrologia* 30 (1993) 67–73.
- [7] E. Schmidt, W. Beckmann, E. Pohlhausen, Das Temperatur- und Geschwindigkeitsfeld vor einer Wärme abgebenden senkrechten Platte bei natürlicher Konvektion, *Forsch. Arb. Ing.-Wes* 1 (1930) 391–406.
- [8] M. Gläser, Change of the apparent mass of weights arising from the temperature differences, *Metrologia* 36 (1999) 183–197.
- [9] G. Mana, C. Palmisano, A. Perosino, S. Pettorruso, A. Peuto, G. Zosi, Convective forces in high precision mass measurements, *Meas. Sci. Technol.* 13 (2002) 13–20.
- [10] H. Schlichting, K. Gersten, *Boundary Layer Theory*, 8th ed., Springer-Verlag, Berlin, 2000, pp. 265–275.
- [11] F.P. Incropera, D.P. DeWitt, *Fundamentals of Heat and Mass Transfer*, fourth ed., John Wiley & Sons, New York, 1996, pp. 482–505.
- [12] F.M. White, *Viscous Fluid Flow*, second ed., McGraw-Hill, Inc., New York, 1991, pp. 324–326.
- [13] I. Pop, H.S. Takhar, Free convection from a curved surface, *Z. Angew. Math. Mech.* 73 (1993) 534–539.
- [14] S. Ostrach, An analysis of laminar free convection flow and heat transfer about a flat plate parallel to the direction of the generating body force, NACA Report 1111, 1953.
- [15] R.S. Davis, Equation for the determination of the density of moist air (1981/1991), *Metrologia* 29 (1992) 67–70.
- [16] Guide to the expression of uncertainty in measurement, Geneva, International organisation for standardisation, 1993, p. 101.